Journal of Applied Polymer Science

Surface Modification of $BaTiO_3$ Inclusions in Polydicyclopentadiene Nanocomposites for Energy Storage

Sean P. Culver, Christopher W. Beier, Jessica P. Rafson, Richard L. Brutchey
Department of Chemistry, University of Southern California, Los Angeles, California 90089
S. P. Culver and C. W. Beier contributed equally to this work.
Correspondence to: R. L. Brutchey (E - mail: brutchey@usc.edu)

ABSTRACT: A new nanocomposite system displaying high breakdown strength, improved permittivity, low dielectric loss, and high thermal stability is presented. Free-standing nanocomposite films were prepared via a solvent-free *in-situ* polymerization technique whereby 5 vol % $BaTiO_3$ (BT) nanocrystals with tailored surface chemistry were dispersed in dicyclopentadiene (DCPD) prior to initiation of ring opening metathesis polymerization by a second generation Grubbs catalyst. The relative permittivity was enhanced from 1.7 in the neat poly(DCPD) film to a maximum of 2.4 in the composite, while the dielectric loss tangent was minimized below 0.7%. Surface modification of the BT nanocrystals mitigated reduction in breakdown strength of the resulting nanocomposites such that only a 13% reduction in breakdown strength was observed relative to the neat polymer films. © 2013 Wiley Periodicals, Inc. J. Appl. Polym. Sci. **2014**, *131*, 40290.

KEYWORDS: composites; nanoparticles; nanocrystals; ring-opening metathesis; surfaces; interfaces

Received 13 November 2013; accepted 12 December 2013
DOI: 10.1002/app.40290

INTRODUCTION

Recently, there has been significant interest in the development of capacitors that can meet energy storage needs that require high breakdown strength, low dielectric loss, and high thermal stability. By using a nanocomposite approach, it has become possible to take advantage of the solution processability and high breakdown strength of polymers combined with the high permittivity of inorganic nanoparticles toward achieving this goal. Among the available inorganic filler materials for nanocomposite capacitors, $BaTiO_3$ (BT) has become prevalent because of its high dielectric constant.[1,2] As a result, the addition of BT nanocrystals into polymer matrices has been shown to systematically increase composite permittivity. The main drawback of using inorganic fillers is that their inclusion, even at low volume loadings ($\leq$5 vol %), often leads to a cataclysmic reduction of the nanocomposite breakdown strength, lessening any benefit achieved from increased permittivity in terms of energy storage capability.[3–6]

Polydicyclopentadiene (pDCPD) is a crosslinked thermoset polymer that can be prepared via ring opening metathesis polymerization of dicyclopentadiene (DCPD) with Grubbs catalyst.[7–9] Polymerization occurs within the neat monomer (i.e., under solvent-free conditions) and is initiated by very low catalyst loadings (<1 wt %). pDCPD has found widespread application as a result of its high thermal stability and chemical resistance, low water uptake, and excellent mechanical properties.[8,10] In comparison to the well-known thermoplastics polypropylene and polystyrene, pDCPD displays similar permittivity but far better thermal stability (i.e., up to 500°C), thereby extending its use to a variety of high temperature applications.[11,12] While several studies have explored the physical and mechanical attributes of various pDCPD nanocomposites,[13–15] there has been very little study on investigating the dielectric properties. Yin et al. recently published the first known study on the dielectric properties of pDCPD-based nanocomposites, using fumed silica inclusions (10 wt % loading).[12] In their study, neat pDCPD films exhibited breakdown strengths as high as 750 V μm^{-1} with very low dielectric loss (tan $\delta = 0.5\%$). Although the pDCPD/SiO_2 composites demonstrated improvements in the relative permittivity and corona resistance under an AC bias relative to the neat polymer, the DC breakdown strengths were not reported.

To date there have been no studies on incorporating BT inclusions into pDCPD nanocomposites. Herein we investigate the dielectric properties of a model pDCPD/BT nanocomposite. Nanocrystals of BT were surface modified with 10-undecenoic acid to affect the nanocrystal–polymer interface and mitigate losses in breakdown strength. It should be noted that while several studies have probed the effects of phosphonic acid modified inclusions,[4,6] the utility of carboxylic acid ligands has received far less attention. A distinct ligand-dependent effect on the measured breakdown strength was

Additional Supporting Information may be found in the online version of this article.

observed, while enhancements in composite permittivity and low dielectric loss tangents were maintained.

EXPERIMENTAL

All manipulations were performed under a nitrogen atmosphere using dry, air-free solvents throughout. BT nanocrystals (≥99.9% trace metals basis; U.S. Research Nanomaterials, Inc.), 10-undeceneoic acid (99%; Alfa Aesar), DCPD (95%; Alfa Aesar), [1,3-bis(2,4,6-trimethylphenyl)-2-imidazolidinylidene]dichloro(phenylmethylene) (tricyclohexylphosphine)ruthenium (Grubbs catalyst, second generation; Materia, Inc.), potassium permanganate (98%; Alfa Aesar), oxalic acid dihydrate (98%; Alfa Aesar), and concentrated sulfuric acid (EMD Chemicals, Inc.) were all used as received.

Surface Modification of BT Nanocrystals

In order to modify the nanocrystal surfaces, 1.58 g (8.60 mmol) of 10-undeceneoic acid was dissolved in 50 mL of dry toluene and added directly to a 100 mL round bottom flask containing 1.0 g of BT nanocrystals. The flask was placed under flowing nitrogen and sonicated for 1 hr at 30°C before the nanocrystals were isolated via centrifugation (6000 rpm for 15 min). The resulting product was washed with toluene (3 × 30 mL) before being dried *in vacuo* (20°C, 0.05 mmHg) for 24 hr, and stored in a dry, air-free environment.

Material Characterization

Transmission electron microscopy (TEM) images were collected on a JEOL JEM-2100 microscope at an operating voltage of 200 kV, which was equipped with a Gatan Orius CCD camera. Samples for TEM analysis were prepared by drop casting suspensions of the nanocrystals in toluene onto ultrathin carbon film supported on 400 mesh copper grids (Ted Pella, Inc.). Scanning electron microscopy (SEM) images were collected on a JEOL JSM-6610LV microscope in high-vacuum mode using an accelerating voltage of 10 kV. Cross-sectional samples were prepared by freeze-fracturing a film, pressing it between two glass plates, and mounting it on top of an aluminum stub. To prevent film charging, a thin layer of carbon was deposited on all films. Fourier transform infrared (FT-IR) spectra were collected on a Bruker Vertex 80v at a scanning interval of 0.5 cm^{-1} with a resolution of 2 cm^{-1} *in vacuo*. Powder X-ray diffraction (XRD) was performed on a Rigaku Ultima IV diffractometer using Cu$K\alpha$ ($\lambda = 1.54$ Å) radiation. For XRD samples of nanocrystalline powder and pDCPD/BT films, the powder or film was placed directly onto a zero diffraction single crystalline silicon substrate (MTI Corporation, Inc.) and patterns were collected in the 20−80 2θ range. All samples for thermogravimetric analysis (TGA) were run on a TA instruments Q50 thermogravimetric analyzer and were dried within the instrument for 30 min under flowing nitrogen at 100°C, followed by ramping to 650°C at a rate of 10°C min^{-1}.

Nanocomposite Preparation

The pDCPD/BT nanocomposites were prepared via an *in situ* polymerization route. In a typical experiment, BT nanocrystals (5 vol %) were added to 1.0 g DCPD. The DCPD was heated to 35°C−40°C to melt the monomer, and then the mixture was sonicated and vortexed. To initiate polymerization, 2 mg (0.2 wt %) of second generation Grubbs catalyst was dissolved in 0.1 mL dry dichloromethane immediately prior to being added to the monomer/nanocrystal mixture. The solution was continually mixed until a slight increase in viscosity was evident (ca., 1 min), and then 0.4 mL of the reaction mixture was removed and immediately cast between two 6″ × 6″ cleaned glass plates and pressed with 50 N of force for 1 hr at 20°C. Film thicknesses were controlled by placing 25.4 μm thick polymer shims (Practi-Shim; Accutrex Products, Inc.) between the glass plates prior to casting. The pressed film was then placed into an oven at 100°C for 24 hr under flowing nitrogen to ensure complete polymerization. The film was slowly cooled to room temperature under flowing nitrogen for 2 hr before removal from the oven and lifting the film. Upon reaching room temperature, the free-standing film was lifted from the glass plates by immersing them into deionized water. The film was blotted dry and cut into squares 1.27 × 1.27 cm^2 in size and stored under nitrogen. Film thickness ranged between 20 and 40 μm as measured by a custom metrology tool with ±1 μm accuracy. Glass plates were cleaned by immersion in a very dilute solution of $KMnO_4$/H_2SO_4 (1 : 1 approximate molar ratio) for a minimum of 48 hr. The plates were removed from the solution, rinsed with deionized water, and then soaked in a dilute aqueous solution of oxalic acid for 30 min. The plates were removed from the oxalic acid bath, rinsed with deionized water, dried under flowing nitrogen, and used immediately.

Nanocomposite Characterization

In order to measure the capacitance and dielectric loss of the as-prepared free standing films, a custom dielectric testing station comprised of flat circular aluminum electrodes was used. The film was placed directly between the two electrodes and pressed, forming a parallel plate geometry (17 mm^2 plate area). Capacitance and loss tangents were measured on an Agilent 4294A impedance analyzer with a frequency sweep of 1 kHz–2 MHz. Dielectric breakdown measurements were performed using a gold plated hemispherical rod (1 mm in diameter) that made direct contact with the pDCPD/BT film. Upon contact, the film was immersed into a mineral oil bath, then subjected to a DC negative polarity bias at a linear ramp rate of 2500 V s^{-1} (Bertan 225, 20 kV DC power supply), connected to a high-voltage probe (Tektronix P6015A; Tektronix, Inc.), and monitored by an oscilloscope (Tektronix TDS 2004C; Tektronix, Inc). Breakdown events were indicated by a spontaneous increase in current. One breakdown test was performed per 1.6 cm^2, with 15−20 independent measurements conducted for each nanocomposite. The points for breakdown tests were chosen at random, and the thickness was measured after each breakdown event within close proximity to the failure site.

RESULTS AND DISCUSSION

BT Nanocrystal Surface Modification

Powder XRD confirmed the crystallinity and phase purity of the BT nanocrystals, which were determined to be in the cubic perovskite phase with a measured lattice constant of $a = 4.04 \pm 0.05$ Å (JCPDS no. 75-0215; Figure 1). The nanocrystals were observed to be quasispherical with some anisotropy throughout and possessed an average size of 84 ± 16 nm (Supporting Information Figures S1 and S2). Surface modification of the BT nanocrystals via sonication with 10-undecenoic

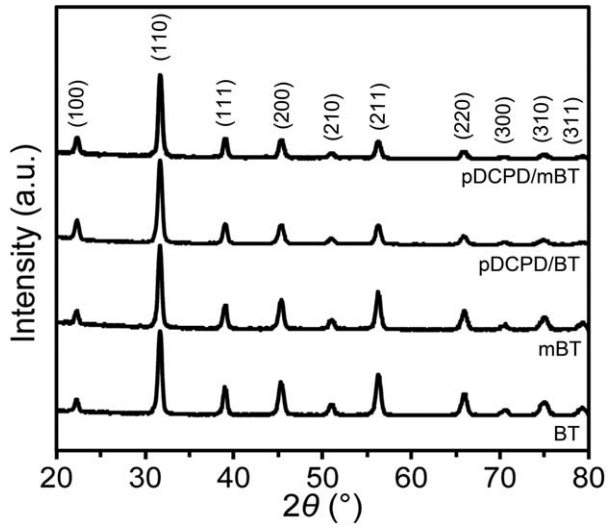

Figure 1. XRD patterns of BT and mBT nanocrystals, and pDCPD/BT and pDCPD/mBT nanocomposite films.

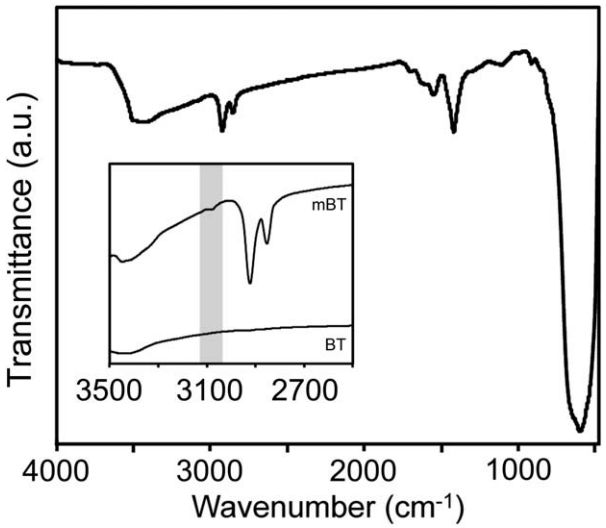

Figure 2. FT-IR spectrum of mBT nanocrystals. Inset: Zoomed in FT-IR spectra of BT and mBT nanocrystals with the alkenyl C—H stretching band highlighted for clarity.

acid (an unsaturated carboxylic acid) was employed toward affecting the resultant nanocomposite properties, hereafter referred to as mBT. Sonication allows for a more rapid and lower temperature surface modification procedure as compared with traditional methods.[16–19] Functionalization of the nanocrystals was confirmed by FT-IR spectroscopy (Figure 2). The presence of strong alkyl ν(C—H) stretching bands at 2960 and 2860 cm^{-1} and a weaker alkenyl ν(C—H) band at 3080 cm^{-1} verified binding of the carboxylic acid (see inset). The symmetric $\nu(CO_2)$ stretching band of the carboxylic acid was located at 1421 cm^{-1}, while the asymmetric $\nu(CO_2)$ stretching band was found at 1548 cm^{-1}. The associated separation between the symmetric and asymmetric bands can be used to reveal the carboxylate binding mode.[20–22] The observed difference of 127 cm^{-1} suggests bidentate chelation by the carboxylate moieties on the nanocrystal surface. After extensive solvent rinsing, there remained approximately 81% of a theoretical monolayer of 10-undeceneoic acid on the surface, as determined by TGA [Figure 3(a)] and calculated surface area values, assuming an area of approximately 0.21 nm^2 for each carboxylate group.[23,24]

Nanocomposite Preparation and Physical Properties

Cross sectional SEM micrographs of the nanocomposite films confirm the measured film thicknesses—all films were determined to be between 20 and 40 μm (Supporting Information Figure S3). The neat pDCPD films were extremely flexible, optically clear, and displayed a faint yellow hue as a result of the ruthenium catalyst. Upon addition of 5 vol % BT and mBT, the nanocomposites became opaque yet maintained their excellent mechanical properties, as the composites remained both flexible and fracture free (Supporting Information Figure S4). The very low viscosity of the DCPD monomer ensured effective mixing of the nanocrystal inclusions. Once surface modified, the BT nanocrystals demonstrated improved processability and a reduction in agglomerate size in the resultant films was observed by SEM (Supporting Information Figure S3). No gross agglomerates on the order of 10–25 μm were noted in the pDCPD/mBT films, as were found in the pDCPD/BT films. Furthermore, XRD patterns of the nanocomposite films confirmed that the

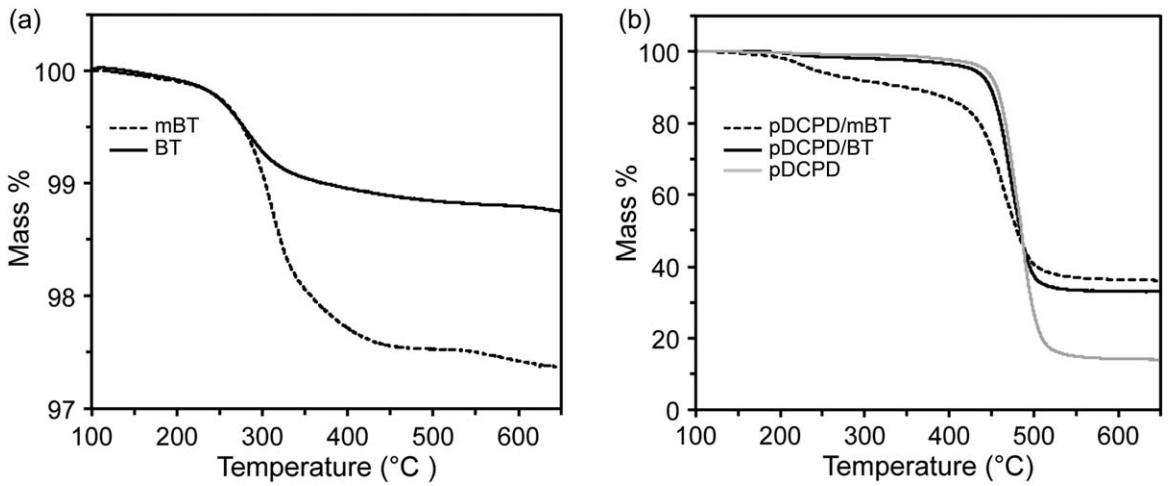

Figure 3. TGA curves for (**a**) BT and mBT nanocrystals and (**b**) neat pDCPD, pDCPD/BT, and pDCPD/mBT free-standing films.

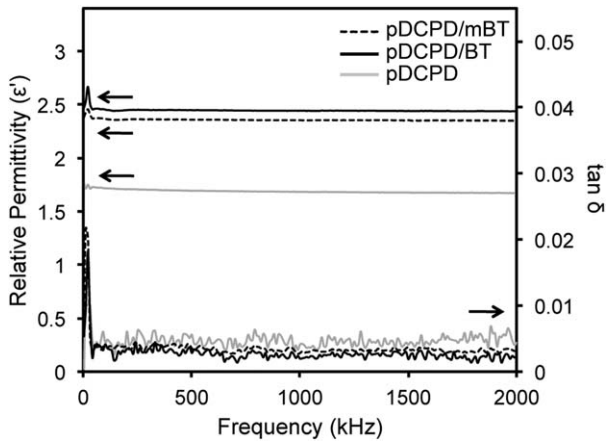

Figure 4. Relative permittivity and dielectric loss tangent (tan δ) of pDCPD, pDCPD/BT, and pDCPD/mBT free-standing films as a function of frequency (25°C).

BT nanocrystals were phase pure after processing, with no indication of $BaCO_3$ formation.

In regards to thermal stability, the pDCPD/BT composites (referring to both the modified and unmodified BT nanocomposites) were quite thermally robust, as confirmed by TGA. Figure 3(b) demonstrates that addition of the unmodified nanocrystals had no effect on the thermal properties relative to the neat pDCPD films, which possessed a decomposition onset at 450°C under nitrogen. On the other hand, the pDCPD/mBT nanocomposite displayed slightly reduced thermal stability, with a decomposition onset occurring at 390°C. The lower temperature mass loss is largely attributed to the ω-olefin functionalized BT nanocrystals crosslinking with the pDCPD matrix during polymerization.[25–27] The crosslinking disrupts the extended pDCPD crosslinked network, likely producing regions with reduced thermal stability. Additionally, a small amount of mass loss stems from the decomposition of the unreacted surface bound ligands, consistent with the decomposition onset obtained for the mBT nanocrystals [Figure 3(a)].

Nanocomposite Dielectric Properties

The relative permittivity and dielectric loss of the free-standing nanocomposite films were measured in a frequency range of 1 kHz–2 MHz (Figure 4). The permittivity of the pDCPD/BT nanocomposites was higher than the neat pDCPD films at all frequencies tested. For example, the relative permittivity of pDCPD was 1.7 at 1.0 MHz and increased to 2.4 after the addition of 5 vol % BT. Upon addition of 5 vol % mBT, the nanocomposite retained a permittivity of 2.3 at 1 MHz. Importantly, dielectric loss tangents remained below 0.7% for all free-standing films at frequencies up to 2 MHz. Dielectric loss tangent below 1% is generally desirable for capacitor applications, as it reduces the likelihood for leakage currents that facilitate premature breakdown at low electric fields.[28] Therefore, the low dielectric losses observed for all pDCPD nanocomposites in this study are practically competitive for low loss applications.

Dielectric breakdown strengths were calculated using a two-parameter Weibull distribution function with the cumulative probability of breakdown, P, defined as:

$$P(V)=1-\exp\left[-\left(\frac{V}{E_{BD}}\right)^{\beta}\right]$$

where V is the measured breakdown voltage, E_{BD} is the breakdown strength at 63.2% cumulative probability, and β is the shape parameter which indicates the width of the distribution. Distributions are provided in Figure 5. The breakdown strength of the neat pDCPD film was found to be 541 V μm^{-1}. Upon inclusion of 5 vol % of BT nanocrystals, the breakdown strength drops more than 25% to 405 V μm^{-1}, which is consistent with previous reports of BT-based nanocomposites.[3,29,30] Traditionally, BT-based nanocomposites display a significant decrease in breakdown strength even at low loadings.[29] For example, Dang et al. prepared polyimide/BT nanocomposites and observed a 40% decrease in breakdown strength at 5 vol % loading, with improved energy storage properties only achieved at loadings exceeding 30 vol %.[3,30] Almadhoun et al. found that the incorporation of <100 nm BT in poly(-vinylidenefluoride-*co*-trifluoroethylene) caused the breakdown strength to fall 25% from 225 to 170 V μm^{-1} at 5 vol % loading.[31] In their study, by hydroxylating the surface of the nanoinclusions, the authors were able to mitigate the decrease to 200 V μm^{-1} at the same loading via weak interfacial dipole interactions. Furthermore, Kim et al. were able to limit the decrease in breakdown strength at 5 vol % in a similar ferroelectric polymer system [i.e., poly(vinylidenefluoride-co-hexafluoropropylene)] by surface modifying the BT inclusions with pentafluorobenzyl phosphonic acid.[6] More recently, Beier et al. demonstrated that the incorporation of a homogenous dispersion of approximately 10 nm $Ba_{0.7}Sr_{0.3}TiO_3$ nanocrystals in a polyimide matrix enhanced the breakdown strength from 240 to ~290 V μm^{-1} at 5 vol % loading.[32] Herein, surface modification of BT nanocrystals with 10-undecenoic acid resulted in nanocomposites with improved high voltage endurance relative to the unmodified inclusions and exceptionally high breakdown strength overall. The pDCPD/mBT nanocomposite displayed a breakdown strength of 468 V μm^{-1}, representing only a 13% reduction relative to the neat polymer films, which corresponds to

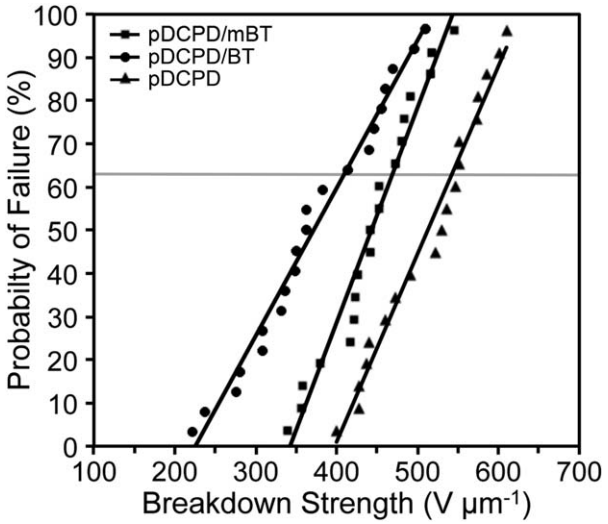

Figure 5. Two-parameter Weibull plots of pDCPD, pDCPD/BT, and pDCPD/mBT free-standing films. *Gray line* represents the Weibull breakdown strength at 63.2% cumulative probability.

a competitive reduction in breakdown strength as compared with previous nanocomposite systems with comparable volume loadings. The presence of a non-polar organic shell not only improves nanocrystal dispersion, but likely mitigates the permittivity offset between the host matrix and the inclusions, thereby dampening the effects of localized field enhancements.[4,5,33,34] In this system, surface modification has effectively been shown to mitigate substantial drops in breakdown strength at low loadings, while retaining the beneficial dielectric properties induced by the high permittivity BT nanocrystals.

CONCLUSIONS

Nanocrystals of BT were successfully dispersed in pDCPD films via an *in-situ* polymerization route to investigate the effects of inclusion surface modification on the dielectric properties of a novel pDCPD/BT nanocomposite. At 5 vol % BT nanocrystal loading, the relative permittivity of the nanocomposites increased from 1.7 in the neat pDCPD film to 2.4 in the pDCPD/BT composite, while low dielectric loss tangents (<0.7%) were obtained for all compositions up to 2 MHz. Furthermore, the pDCPD/mBT nanocomposite exhibited a breakdown strength of 468 V μm^{-1}, which represented only a 13% reduction from that of the neat pDCPD films. Therefore, surface modification of the BT nanocrystal inclusions with 10-undecenoic acid was shown to enhance breakdown strengths relative to the unmodified inclusions, while maintaining increased permittivity, low dielectric loss, and excellent thermal stability. Although further optimization of the polymer dielectric properties is required to achieve higher filler loadings, pDCPD represents a promising polymer matrix toward improving nanocomposite-based energy storage devices.

ACKNOWLEDGMENTS

This work is supported by the Department of Energy Office of Basic Energy Sciences under Grant no. DE-FG02-11ER46826. We thank the Resource Center for Medical Ultrasonic Transducer Technology at USC for use of their impedance equipment, and Materia, Inc. for providing us with Grubbs catalyst.

REFERENCES

1. Lines, M. E.; Glass, A. M. Oxford Classic Texts in the Physical Sciences; Oxford University Press: New York, **2001**.
2. Newnham, R. E., Cross, L. E. *MRS Bull.* **2011**, *30*, 845.
3. Dang, Z. M.; Lin, Y. Q.; Xu, H. P.; Shi, C. Y.; Li, Y. S.; Bai, J. *Adv. Funct. Mater.* **2008**, *18*, 1509.
4. Kim, P.; Jones, S. C.; Hotchkiss, P. J.; Haddock, J. N.; Kippelen, B.; Marder, S. R.; Perry, J. W. *Adv. Mater.* **2007**, *19*, 1001.
5. Barber, P.; Balasubramanian, S.; Anguchamy, Y.; Gong, S.; Wibowo, A.; Gao, H.; Ploehn, H. J.; Zur Loye, H. C. *Materials* **2009**, *2*, 1697.
6. Kim, P.; Doss, N. M.; Tillotson, J. P.; Hotchkiss, P. J.; Pan, M. J.; Marder, S. R.; Li, J.; Calame, J. P.; Perry, J. W. *ACS Nano* **2009**, *3*, 2581.
7. Slugovc, C. *Macromol. Rapid Commun.* **2004**, *25*, 1283.
8. Grubbs, R. H. Handbook of Metathesis; Wiley-VCH: Weinheim, Germany, **2003**.
9. Kissin, Y. V. Kirk-Othmer Encyclopedia of Chemical Technology, Wiley: New Jersey, **2005**.
10. Grubbs, R. H. *Tetrahedron* **2004**, *60*, 7117.
11. Rabuffi, M.; Picci, G. *IEEE T. Plasma Sci.* **2002**, *30*, 1939.
12. Yin, W.; Kniajanski, S.; Amm, B. Conference Record of the 2010 IEEE International Symposium on Electrical Insulation (ISEI). **2010**.
13. Simons, R.; Guntari, S. N.; Goh, T. K.; Qiao, G. G.; Bateman, S. A. *J. Polym. Sci. Part A: Polym. Chem.* **2012**, *50*, 89.
14. Jeong, W.; Kessler, M. R. *Chem. Mater.* **2008**, *20*, 7060.
15. Yoonessi, M.; Toghiani, H.; Kingery, W. L.; Pittman, C. U. *Macromolecules* **2004**, *37*, 2511.
16. Xu, C.; Xu, K.; Gu, H.; Zheng, R.; Liu, H.; Zhang, X.; Guo, Z.; Xu, B. *J. Am. Chem. Soc.* **2004**, *126*, 9938.
17. Shultz, M. D.; Reveles, J. U.; Khanna, S. N.; Carpenter, E. E. *J. Am. Chem. Soc.* **2007**, *129*, 2482.
18. Huang, W.; Lin, Y.; Taylor, S.; Gaillard, J.; Rao, A. M.; Sun, Y. P. *Nano Lett.* **2002**, *2*, 231.
19. Koshio, A.; Yudasaka, M.; Zhang, M.; Iijima, S. *Nano Lett.* **2001**, *1*, 361.
20. Zhang, L.; He, R.; Gu, H. C. *Appl. Surf. Sci.* **2006**, *253*, 2611.
21. Mielczarski, J. A.; Cases, J. M.; Bouquet, E.; Barres, O.; Delon, J. F. *Langmuir* **1993**, *9*, 2370.
22. Mielczarski, J. A.; Cases, J. M. *Langmuir* **1995**, *11*, 3275.
23. Allara, D. L.; Nuzzo, R. G. *Langmuir* **1985**, *1*, 52.
24. Sahoo, Y.; Goodarzi, A.; Swihart, M. T.; Ohulchanskyy, T. Y.; Kaur, N.; Furlani, E. P.; Prasad, P. N. *J. Phys. Chem. B* **2005**, *109*, 3879.
25. Skaff, H.; Ilker, M. F.; Coughlin, E. B.; Emrick, T. *J. Am. Chem. Soc.* **2002**, *124*, 5729.
26. Tavasoli, E.; Guo, Y.; Kunal, P.; Grajeda, J.; Gerber, A.; Vela, J. *Chem. Mater.* **2012**, *24*, 4231.
27. Liu, X.; Basu, A. *J. Organomet. Chem.* **2006**, *691*, 5148.
28. Dissado, L. A.; Fothergill, J. C. IEE Materials and Devices Series 9; Peter Peregrinus Ltd.: London, United Kingdom, **1992**.
29. Khalil, M. S. *IEEE T. Dielect. El. In.* **2000**, *7*, 261.
30. Feng, Y.; Yin, J.; Chen, M.; Liu, X.; Li, G. Dielectric Properties of PI/BaTiO3 with Disparate Inorganic Content. In 6th International Forum on Strategic Technoology, Heilongjian, China, August 22–24, 2011; IEEE: Piscataway, NJ, **2011**; pp 226–229.
31. Almadhoun, M. N.; Bhansali, U. S.; Alshareef, H. N. *J. Mater. Chem.* **2012**, *22*, 11196.
32. Beier, C. W.; Sanders, J. M.; Brutchey, R. L. *J. Phys. Chem. C* **2013**, *117*, 6958.
33. Jung, H. M.; Kang, J. H.; Yang, S. Y.; Won, J. C.; Kim, Y. S. *Chem. Mater.* **2010**, *22*, 450.
34. Beier, C. W.; Cuevas, M. A.; Brutchey, R. L. *Langmuir* **2009**, *26*, 5067.